Supporting information

Table of Content

Method of Microkinetic modelings

Microkinetic modelings, as also reported in our previous work [1], are conducted to determine the main reaction pathways, rate-determining steps, and surface species coverage[2] [3-5]. The results of DFT frequency can be used to calculate the pre exponential factor of elementary reaction. The forward reaction pre index factor (ν_{forward}) and the reverse reaction pre index factor (ν_{reverse}) are calculated using Eq. (S1) and (S2) respectively:

$$\nu_{\text{for}} = \frac{\prod_{m=1}^{N} \nu_m^{IS}}{\prod_{n=1}^{N} \nu_n^{TS}} \tag{S1}$$

$$\nu_{\text{rev}} = \frac{\prod_{m=1}^{N} \nu_m^{FS}}{\prod_{n=1}^{N} \nu_n^{TS}} \tag{S2}$$

ν_m^{IS} is the frequency of the initial state of the reaction; ν_n^{TS} is the frequency of the transition state (the saddle point in the reaction); ν_m^{FS} is the frequency of the final state of the reaction.

The reaction rate constant of elementary reaction can be calculated according to Arrhenius formula through Eq. (S3) [6]:

$$k = \mathrm{A}\exp(-\frac{E}{RT}) \tag{S3}$$

wherein the k stands for reaction rate constant; A stands for pre-exponential factor; E stands for reaction energy barrier (calculated by DFT); R is the molar gas constant; T is for temperature.

In addition, the pre exponential factor of the desorption step is calculated using Eq. (S4) [7,8].

$$\mathrm{A}=\frac{k_B \mathrm{T}}{h} \mathrm{e}^{n_1} \left(\frac{P^\theta}{RT}\right)^{1-n} \exp\left(\frac{\Delta_r S_m^\theta\left(P^\theta\right)}{R}\right) \tag{S4}$$

k_B is the Boltzmann constant; h is Planck's constant; P^θ represents standard partial pressure; $\Delta_r S_m^\theta$ is the standard molar entropy difference before and after desorption; n_1 represents the sum of reaction coefficients of gaseous reactants; n is the sum of all the reactants.

The Reaction rate constant of the adsorption step is calculated by Eq. (S5) [9]:

$$k_{ad} = s_0 P_i A_i \Big/ \sqrt{2\pi m_i k_B T} \quad \text{(S5)}$$

Among them, k_{ad} represents the adsorption rate; s_0 represents the viscosity coefficient of the adsorbed species i; P_i (pa) represents the gas phase partial pressure of the adsorbed species i; A_i (m^2) represents the adsorption area; m_i (kg) represents the molecular weight of the adsorbed species i; k_B represents the Boltzmann constant.

The reaction rate equation is solved by using Matlab. Reaction rate and surface species coverage.

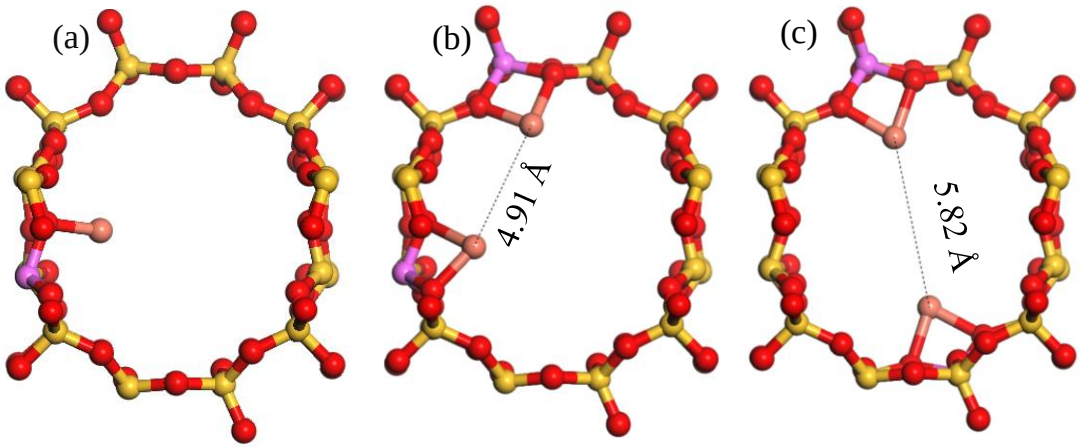

Figure S1. Optimized Cu-BEA models with diverse Cu active site motifs (a) Z^a-Cu; (b) Z^b-Cu; (c) Z^c-Cu site; Si (yellow), O (red), N (blue), Al (pink), Cu (orange).

	monomeric $[Cu]^+$
Route A1	$Z^a\text{-}Cu\text{-}N_2O \rightarrow TSA1$
	$TSA1 \rightarrow Z^a\text{-}Cu\text{-}O + N_2$
Route A2	$Z^a\text{-}Cu\text{-}O + C_3H_8 \rightarrow TSA2$
	$TSA2 \rightarrow Z^a\text{-}Cu\text{-}OH\text{-}C_3H_7$
Route A3	$Z^a\text{-}Cu\text{-}OH\text{-}C_3H_7 \rightarrow TSA3$
	$TSA3 \rightarrow Z^a\text{-}Cu\text{-}H_2O + C_3H_6$
Part2	**dimeric $[Cu\text{-}Cu]^{2+}$**
Route B1	$Z^b\text{-}Cu_2\text{-}N_2O \rightarrow TSB1$
	$TSB1 \rightarrow Z^b\text{-}Cu\text{-}O\text{-}Cu + N_2(g)$
Route B2	$Z^b\text{-}Cu\text{-}O\text{-}Cu + C_3H_8 \rightarrow TSB2$
	$TSB2 \rightarrow Z^b\text{-}Cu_2\text{-}C_3H_7\text{-}OH$
Route B3	$Z^b\text{-}Cu_2\text{-}C_3H_7\text{-}OH \rightarrow TSB3$
	$TSB3 \rightarrow Z^b\text{-}Cu_2\text{-}C_3H_6\text{-}H_2O$
Part3	**distant $[Cu]^+$—$[Cu]^+$**
Route C1	$Z^c\text{-}Cu_2\text{-}N_2O \rightarrow TSC1$
	$TSC1 \rightarrow Z^c\text{-}Cu_2\text{-}O + N_2(g)$
Route C2	$Z^c\text{-}Cu_2\text{-}O + C_3H_8 \rightarrow TSC2$
	$TSC2 \rightarrow Z^c\text{-}Cu_2\text{-}C_3H_7\text{-}OH$
Route C3	$Z^c\text{-}Cu_2\text{-}C_3H_7\text{-}OH \rightarrow TSC3$
	$TSC3 \rightarrow Z^c\text{-}Cu_2\text{-}C_3H_6\text{-}H_2O$

Scheme S1. Schematic reaction for N_2O-ODHP over Z^a-Cu (reaction Route A), Z^b-Cu (reaction Route B) and Z^c-Cu (reaction Route C), respectively**.**

Table S1. Micro-dynamics parameters of the reaction steps over Z^a-Cu, Z^b-Cu and Z^c-Cu site.

Reaction step	Constant	monomeric $[Cu]^+$	dimeric $[Cu\text{-}Cu]^{2+}$	distant $[Cu]^+$—$[Cu]^+$
R1A	K_1	2.30E-10	4.94E-05	5.74E-08
	k_1, s^{-1}	8.87E+10	8.87E+10	1.06E+11
	A_1, s^{-1}	1.00E-15	7.40E+24	1.00E-15
	k_1^{-1}, s^{-1}	3.85E+20	1.80E+15	1.85E+18
	A_1^{-1}, s^{-1}	3.95E+21	2.99E+21	3.23E+21
R2A	k_2, s^{-1}	1.73E+05	5.61E+07	1.34E+08
	A_2, s^{-1}	6.49E+13	6.49E+13	6.49E+13
R3A	K_3	5.63E-13	1.28E-13	2.20E-12
	k_3, s^{-1}	8.87E+10	8.87E+10	1.06E+11
	A_3, s^{-1}	1.00E-15	3.98E+22	1.00E-15
	k_3^{-1}, s^{-1}	1.58E+23	6.94E+23	4.84E+22
	A_3^{-1}, s^{-1}	3.40E+23	2.58E+23	2.78E+23
R4A	K_4	1.46E+15	3.87E+07	3.03E+07
	k_4, s^{-1}	6.73E+11	1.94E+10	1.38E+12
	A_4, s^{-1}	1.29E+12	1.29E+12	1.29E+12
	k_4^{-1}, s^{-1}	4.61E-04	5.00E+02	4.54E+04
	A_4^{-1}, s^{-1}	1.70E+13	1.70E+13	1.70E+13
R5A	K_5	4.93E+00	5.96E-01	1.39E+07
	k_5, s^{-1}	7.27E-03	5.28E+01	7.22E+12
	A_5, s^{-1}	7.82E+14	7.82E+14	1.39E+07
	k_5^{-1}, s^{-1}	9.19E-03	8.85E+01	1.28E+00
	A_5^{-1}, s^{-1}	2.40E+12	2.40E+12	2.40E+12

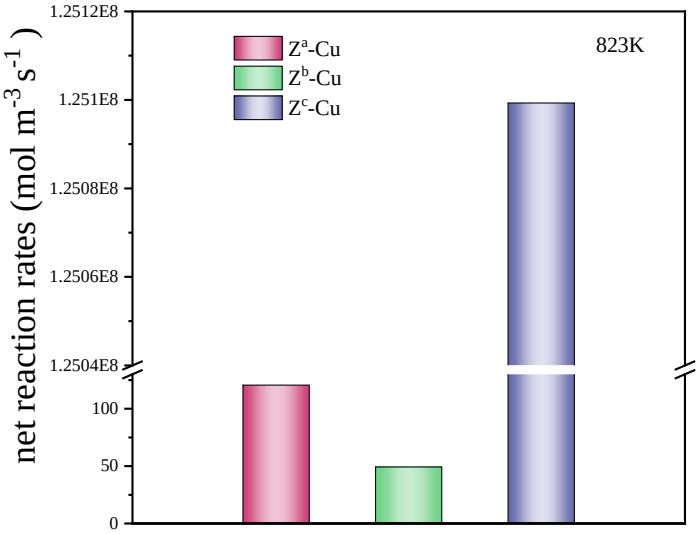

Figure S2. The comparison of net reaction rate over Schematic reaction for N_2O-ODHP over Z^a-Cu, Z^b-Cu and Z^c-Cu site at 823K.

Materials and Methods

The parent H-zeolite catalyst (ZSM-5 and BEA) were commercial products provided by Nankai Catalyst Factory. The catalyst samples of 1%Cu-BEA, 1%Fe-BEA, 1%Fe-ZSM-5 and 1%CuO-SiO_2 with the metal loading of 1 wt.% was prepared via the impregnation method. The metallic nitrates of Fe $(NO_3)_3 \cdot 9H_2O$ and $Cu(NO_3)_2 \cdot 3H_2O$ as well as SiO_2 were purchased from Shanghai Aladdin Biochemical Technology Company.

Specifically, the impregnation procedure includes following steps: i) initially, 5 g H-zeolites or SiO_2 was mixed with desired amounts of metal nitrates in 300 mL round-bottom flask; ii) after adding 200 mL deionized water, the solution was stirring at 90 ºC for 4h over the rotary vacuum evaporator; iii) the product can be eventually obtained after the further calcination at 550 °C for 6 h.

The catalyst activity measurement was conducted over a quartz fixed-bed reactor (id = 7 mm, od = 9 mm, L = 475 mm) at T = 550 ºC. The catalyst samples of 0.1 g (40~60 mesh) were loaded into the reactor, under the atmosphere of 10 vol% C_3H_8, 10 vol% N_2O being balanced by He. The gas hourly space velocity (GHSV) was set to be 12,000 h^{-1}, which corresponds to a flow rate of 21 mL min^{-1}. Before the activity measurement, the samples were initially pretreated at 550 °C for 1h with He of 30 mL min^{-1}. The outlet gases were on-line analyzed by gas chromatograph (Shimadzu GC-2014) which was equipped with TCD/FID detector, and Propark Q and 13X molecular sieve column.

Reference

1. Xu, R.; Liu, N.; Dai, C.; Li, Y.; Zhang, J.; Wu, B.; Yu, G.; Chen, B., H_2O - Built Proton Transfer Bridge Enhances Continuous Methane Oxidation to Methanol over Cu - BEA Zeolite. *Angew. Chem. Int. Ed.* **2021,** *60*, 16634-16640.
2. Zhou, Z.; Qin, B.; Li, S.; Sun, Y., A DFT-based microkinetic study on methanol synthesis from CO_2 hydrogenation over the In_2O_3 catalyst. *Phys Chem Chem Phys* **2021,** *23*, 1888-1895.
3. Liu, N.; Yuan, X.; Zhang, R.; Xu, R.; Li, Y., Mechanistic insight into selective catalytic combustion of acrylonitrile (C_2H_3CN): NCO formation and its further transformation towards N_2. *Phys. Chem. Chem. Phys.* **2017,** *19*, 7971-7979.
4. Liu, N.; Yuan, X.; Zhang, R.; Li, Y.; Chen, B., Mechanistic insight into selective catalytic combustion of HCN over Cu-BEA: influence of different active center structures. *Phys. Chem. Chem. Phys.* **2017,** *19*, 23960-23970.
5. Dixit, M.; Baruah, R.; Parikh, D.; Sharma, S.; Bhargav, A., Autothermal reforming of methane on rhodium catalysts: Microkinetic analysis for model reduction. *Comput. Chem. Eng.* **2016,** *89*, 149-157.
6. Ke, C.; Lin, Z., Density Functional Theory Based Micro- and Macro-Kinetic Studies of Ni-Catalyzed Methanol Steam Reforming. *Catalysts* **2020,** *10*.
7. Liu, N.; Zhang, R.; Chen, B.; Li, Y.; Li, Y., Comparative study on the direct decomposition of nitrous oxide over M (Fe, Co, Cu)–BEA zeolites. *J. Catal.* **2012,** *294*, 99-112.
8. Gokhale, A. A.; Kandoi, S.; Greeley, J. P.; Mavrikakis, M.; Dumesic, J. A., Molecular-level descriptions of surface chemistry in kinetic models using density functional theory. *Chem. Eng. Sci.* **2004,** *59*, 4679-4691.
9. Cai, Q.-X.; Wang, J.-G.; Wang, Y.-G.; Mei, D., Mechanistic insights into the structure-dependent selectivity of catalytic furfural conversion on platinum catalysts. *AlChE J.* **2015,** *61*, 3812-3824.